Letter

optica

Organic Solar Cells as High Speed Data Detectors for Visible Light Communication

SHUYU ZHANG[1,3†], DOBROSLAV TSONEV[2,†], STEFAN VIDEV[2], SANJAY GHOSH[1], GRAHAM A. TURNBULL[1,*], IFOR D.W. SAMUEL[1,*] AND HARALD HAAS[2,*]

[1]Organic Semiconductor Centre, SUPA, School of Physics and Astronomy, University of St Andrews, St Andrews, Fife KY16 9SS, UK
[2]Institute for Digital Communications, LiFi R&D Centre, University of Edinburgh, Edinburgh EH9 3JL,UK
[3] School of Information Science and Technology, Fudan University, Shanghai, 200433, China PR
*Corresponding authors: gat@st-andrews.ac.uk; idws@st-andrews.ac.uk; h.haas@ed.ac.uk

Received XX Month XXXX; revised XX Month, XXXX; accepted XX Month XXXX; posted XX Month XXXX (Doc. ID XXXXX); published XX Month XXXX

We show that solar cells, widely used in portable devices for power generation, can simultaneously extract a high-speed data signal in an optical wireless communication link. This paper reports the first use of an organic solar cell as an energy-harvesting receiver for visible light communications (VLC). While generating maximum power in the cell, the communication link can deliver a data-rate of 34.2 Mbps with a bit error rate of 4.08×10^{-4} using an implementation of orthogonal frequency division multiplexing. This approach could lead to printed optical data receivers in future eco-friendly VLC systems. Simultaneous functions of data communication and energy harvesting have great implications for the connectivity of future smart devices, many of which could become self-powered units as part of the 'Internet of Things'. © 2015 Optical Society of America

OCIS codes: *(060.4510) Optical communications; (040.5350) Photovoltaic; (160.4890) Organic materials.*

http://dx.doi.org/10.1364/optica.99.099999

The looming radio frequency (RF) spectrum crunch has prompted research into alternative regions of the electromagnetic (EM) spectrum for future wireless communication systems. The infrared and visible light region of the EM spectrum are of particular interest since the vast amount of available bandwidth is unregulated and free of electromagnetic interference (EMI). The growing infrastructure of LED lighting offers a particular opportunity for visible light communications (VLC) with power-efficient dual-use sources, which provide simultaneous illumination and very high rate wireless data transmission [1-5]. While VLC data links normally use photodiode (PD) receivers [5] (either positive-intrinsic-negative (PIN) PDs or avalanche PDs), there is a parallel opportunity for duality by using instead a solar cell for simultaneous energy harvesting and data detection. Wang *et al.* recently showed that a standard commercial multi-crystalline silicon solar panel could be used for this dual purpose, to receive a data-rate of 11.84 Mbps while generating approximately 2 mW of electrical power [6, 7]. This advance implies that it could be possible for any piece of electronic equipment with an integrated solar cell to engage in high-speed data communication while utilising the energy from the light signal or ambient lighting to power the receiver electronics.

However, to unlock the full potential of this approach it would be very attractive to use an alternative solar cell technology that could be more easily integrated on different devices/substrates, or even be mechanically flexible. The field of organic electronics offers these possibilities, and here we report the first use of an organic semiconductor solar cell as the energy-harvesting receiver in an optical wireless data link. When the cell generates maximum power, the communication link is capable of delivering a data-rate of 34.2 Mbps with a bit error rate (BER) of 4.08×10^{-4} using an implementation of orthogonal frequency division multiplexing (OFDM). Such organic solar cells could serve as a future platform for ubiquitous VLC receivers. They can be mass manufactured by roll-to-roll printing on a flexible foil [8], giving the possibility of very inexpensive flexible/conformal panels which could be integrated with an extremely wide range of devices. They offer relatively easy bandgap tuning through the visible which could allow a selective response to wavelengths relevant for VLC. Such receivers could therefore have great implications for the connectivity of future smart devices, from sensor networks to smart clothing, many of which could become self-powered units as part of the 'Internet of Things'.

Organic semiconductor materials have recently attracted much attention in the field of VLC [9-11]. They offer tremendous scope for simple processing and integration on different substrates, and have been used as colour converters to generate white light with a blue LED backlight. A >1 Gbps white light data link was recently demonstrated, taking advantage of the organic material's fast radiative decay rate compared to commercial phosphor colour converters [9]. The same class of materials can also be used as signal detectors for VLC as organic photodiodes. Haigh *et al.* have demonstrated a communication link with a data-rate of 0.75 Mbps by using a poly(3-hexylthiophene) (P3HT): [6,6]- phenyl-C61-butyric acid methyl ester ($PC_{61}BM$) organic photodiode [12]. The data-rate was further improved to 3.8 Mbps by Ghassemlooy *et al.* by improving the bandwidth [13]. However, these organic photodiode receivers operated under an external bias, and so in this mode of operation cannot be used for energy harvesting.

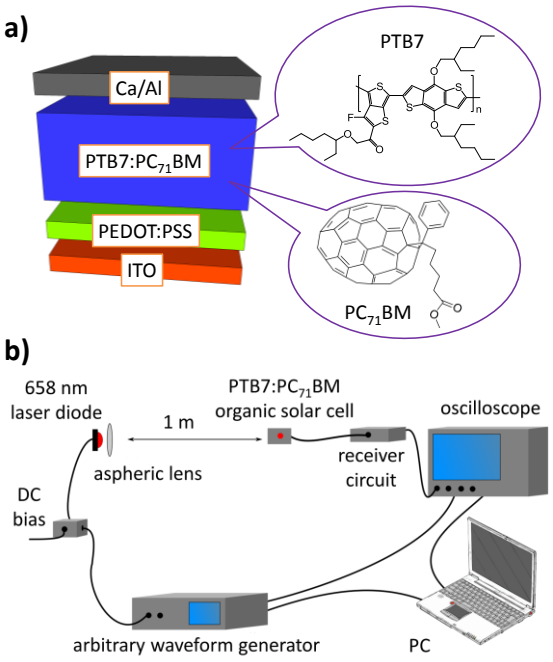

Fig. 1. (a) The device structure of the PTB7:PC71BM solar cell and the molecular structures of PTB7 and PC71BM; (b) the experimental set-up of the VLC data link.

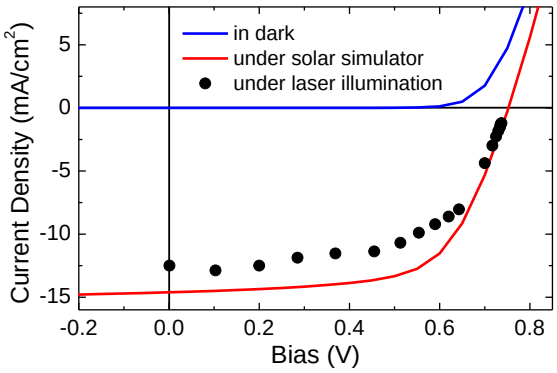

Fig. 2. The current density versus voltage (J-V) curve of the PTB7:PC71BM solar cell in the dark (blue curve), under the illumination of a standard AM 1.5G solar simulator (red curve) and under the illumination of a modulated red laser diode (dots).

In this work we use state-of-the-art organic solar cells based on PTB7:$PC_{71}BM$ material blends (Fig. 1(a)) [14-16] to achieve high power conversion efficiency. We show that data rates of over 34 Mbps are possible while the solar cell maintains its full power generation capabilities. The achieved data rates are an order of magnitude higher than those reported using organic photodiodes.

The device structure of the organic solar cell is shown in Fig. 1(a). Patterned commercial indium tin oxide (ITO) coated glass substrates were cleaned by ultra-sonication in acetone and isopropanol successively for 10 minutes each, followed by an oxygen plasma ashing for 3 minutes. A 40 nm hole injecting layer of poly(3,4-ethylenedioxythiophene):poly(styrenesulfonate) (PEDOT:PSS) was spin-coated on the ITO substrates and annealed on a hotplate at 140 ^{0}C for 10 min to remove the residual water. The 85 nm active layer made of PTB7 and $PC_{71}BM$ in the weight ratio 1:1.5 was spin-coated on top of the PEDOT:PSS layer from chlorobenzene mixed with 3% (v/v) 1,8-diiodooctane (DIO) in a nitrogen-purged glove box. A detailed description of the PTB7:$PC_{71}BM$ blend preparation can be found in Liang *et al.*[13] and He *et al.*[14] A 15 nm calcium and a 100 nm aluminium cathode was then thermally deposited on top in a vacuum chamber at a pressure of 1.5 x 10^{-6} mbar. After the electrode deposition, the devices were encapsulated with a UV optical adhesive and a glass coverslip. The active areas of the devices were 2 x 4 mm^2. The current-voltage characteristics were determined under an illumination intensity of 100 mW/cm^2 in air using an air mass 1.5 global (AM 1.5G) Sciencetech solar simulator and a Keithley 2400 source-measure unit. The illumination intensity was verified with a calibrated monosilicon detector and a KG-5 filter.

Fig. 1(b) shows the experimental set-up of the VLC data link. The conditioned digital signal was passed onto an arbitrary waveform generator (AWG) which outputted an analogue signal. The analogue signal was used to drive a red laser diode (LD) with a narrow emission centred at 658 nm. The light emission of the LD was collimated with an aspheric lens and directed onto the PTB7:$PC_{71}BM$ solar cell. The output of the solar cell was terminated on a custom circuit designed for simultaneous energy harvesting and communication, and the output of the circuit was captured with a digital oscilloscope. The VLC data link used an implementation of OFDM (see **Supplementary Materials**). For the digital signal, a pseudorandom bit sequence was generated and encoded into *M*-ary quadrature amplitude modulation (*M*-QAM) symbols. The *M*-QAM symbols were modulated onto different frequency subcarriers. This was implemented by applying an inverse fast Fourier transform (IFFT) operation on a block of *M*-QAM symbols. The procedure generated a discrete time-domain signal, which was conditioned for transmission by oversampling, pulse shaping and clipping any values outside a predetermined range in order to reduce the peak-to-average power ratio (PAPR) of the modulation signal. All digital processing was implemented in MATLAB.

The incident photon conversion efficiency (IPCE) spectrum of the PTB7:$PC_{71}BM$ solar cell was previously reported in Ref. [16]. PTB7:$PC_{71}BM$ has a broad absorption spectral range. The IPCE values can reach over 50% in the range of 400 to 700 nm, and at the wavelength of the LD, the IPCE is around 70%. Fig. 2 shows the current density versus voltage (J-V) curve of the PTB7:$PC_{71}BM$ solar cell in the dark and under illumination. The blue curve represents the dark current and the red curve represents the J-V curve under the illumination of the AM 1.5G solar simulator. Device parameters such as short-circuit current (J_{SC}), open-circuit voltage (V_{OC}), fill factor (FF) and power conversion efficiency (PCE) can all be obtained from Fig. 2. The fresh PTB7:$PC_{71}BM$ solar cells show a J_{SC} of 14.6 mA/cm^2, a V_{OC} of 0.75 V, a FF of 63.8%, leading to a solar PCE of 7.0%. The values of series resistance (R_S) and shunt resistance (R_{SH}) can also be obtained from the J-V curve. The solar cells exhibit an R_S = 125 Ω and an R_{SH} = 12 kΩ. The small value of R_S indicates good contact between the metal contact and the active layer. The high value of R_{SH} indicates most of the light-generated current contributes to the power generation of the solar cell.

The J-V curve of the solar cell was also measured under the illumination of the LD transmitter (black dots in Fig. 2). The LD was biased at 2.5 V and modulated with a peak-to-peak signal of 0.4 V. The output power of the LD varies from 50 μW at a bias of 2.3 V, to 8.5 mW at a bias of 2.5 V and 14.3 mW at a bias of 2.7 V. For these measurements, the solar cell was connected to a variable load resistor, and by varying the value of the load resistor, the J-V curve in the fourth quadrant was obtained. The branch of the circuit for the

communication signal was open during this measurement. A similar value of V_{OC} and a slightly smaller value of J_{SC} were obtained under the LD illumination.

Table 1 summarises data-rates and generated power when both the energy harvesting circuit branch and the communication circuit branch were connected. It is worth noting that although no external bias is directly applied to the solar cell receiver, different choices of R_L will set different biases across the receiver. The data rates strongly depend on the load resistor. With a load resistance of 5 kΩ, the data-rate is 21.3 Mbps at a BER of 1.59×10^{-3}. As the resistance decreases, the data-rate increases. The data-rate reaches 42.3 Mbps at a BER of 1.10×10^{-3} when the load resistance drops to 200 Ω. In terms of energy harvesting, the circuit branch can generate a maximum power of 0.43 mW (5.4 mW/cm^2) when the load resistance is 600 Ω. At the same time, the communication circuit branch can deliver a data-rate of 34.2 Mbps with a BER of 4.08×10^{-4}. Compared to the power of 0.44 mW generated by the same transmitter without the communication circuit branch, the negligible difference in power generation indicates that the communication circuit branch has no negative impact on the energy harvesting circuit branch.

The organic solar cell receiver system can be described by an equivalent circuit as shown in Fig. 3a. The capacitor C in parallel with R_{SH} captures the internal capacitance of the solar cell, and the inductor L models the inductance of any wire connections to the solar cell [17, 18]. The output of the solar cell contains both DC and AC components. The DC component of the electrical signal, used for energy harvesting, and the AC component, used for communication, are decoupled with a capacitor C_0 (C_0 = 85 nF) and an inductor (RF choke) L_0 (L_0 = 10 μH). The DC current is terminated through a load resistor R_L and the AC current is terminated through the resistor R_C which is matched to the inductor-resistor-capacitor (LRC) equivalent circuit of the solar cell in order to obtain a desired bandwidth and a required signal gain in the receiver system. The frequency response of the receiver system depicted in Fig. 3a can be expressed as:

$$\frac{v(\omega)}{i_{PH}(\omega)} = \frac{R_{LC}R_C\left(R_S + j\omega L + R_{LC}\right)^{-1}\left(\left(j\omega C_0\right)^{-1} + R_C\right)^{-1}}{r^{-1} + j\omega C + R_{SH}^{-1} + \left(R_S + j\omega L + R_{LC}\right)^{-1}} \quad \textbf{(1)}$$

where RLC is the equivalent resistance of the parallel circuit after the inductor L:

Table 1. A summary of the achievable data-rate and the generated power for different values of the load resistance R_L when both the energy harvesting circuit branch and the communication circuit branch are connected to the solar cell. In these results, R_C = 35 Ω. The achievable data-rate is the rate that is targeted to have a BER of 10^{-3}; the actual achieved BER in each measurement is also listed.

R_L [Ω]	Data-rate [Mbps]	BER	P_L [mW] commun. branch connected	P_L [mW] commun. branch open
200	42.3	1.10E-3	0.19	0.19
400	37.8	7.00E-4	0.30	0.34
600	34.2	4.08E-4	0.43	0.44
800	26.8	6.37E-4	0.41	0.43
1k	26.4	7.78E-4	0.38	0.41
2k	22.3	1.23E-3	0.24	0.25
5k	21.3	1.59E-3	0.11	0.11

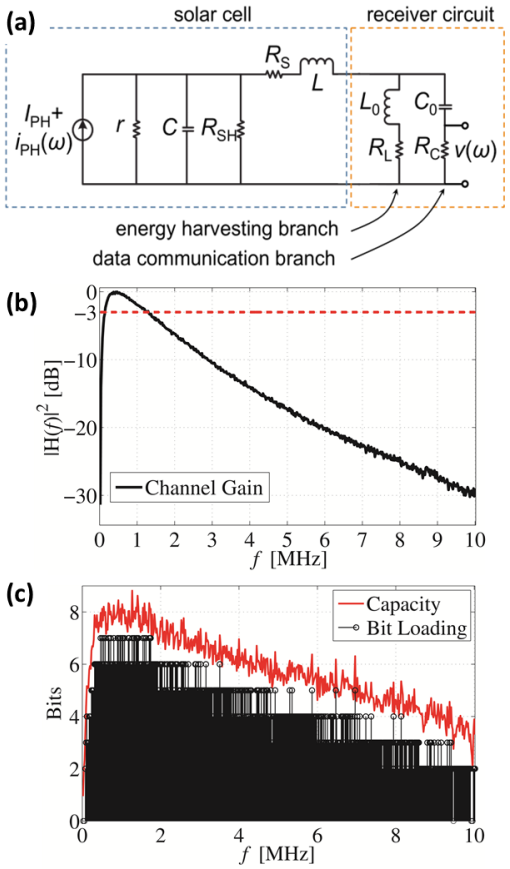

Fig. 3. (a) Solar cell model: equivalent circuit in a configuration for simultaneous energy harvesting and data communication RL and RC are respectively the resistors in the energy harvesting and data communication branches); (b) frequency response and (c) Achieveble cpacaity and optimal bit loading of the solar cell for R_C = 35 Ω and R_L = 200 Ω.

$$R_{LC} = 1/\left(\left(j\omega L_0 + R_L\right)^{-1} + \left(\left(j\omega C_0\right)^{-1} + R_C\right)^{-1}\right) \quad \textbf{(2)}$$

The measured frequency response of the solar cell for R_C = 35 Ω and R_L = 200 Ω, which gave the highest measured data rate of 42.3 Mbps, is shown in Fig. 3b. The frequency profile of the communication system follows a low pass filter response caused by the capacitance of the solar cell. A small portion of the low frequencies in the channel gain curve in Fig. 3b are also attenuated due to the AC-coupling capacitor in the receiver circuit. The 3-dB attenuation frequency of the system is 1.3 MHz. It is interesting to note that the gain of the receiver rolls off gradually, which suggests that a significant amount of bandwidth beyond the 3-dB point may be used for communication. This observation is confirmed by the SNR estimated for a bandwidth of up to 10 MHz using OFDM and error-vector magnitude estimation. The achievable capacity for R_C = 35 Ω and R_L = 200 Ω is shown in Fig. 3c (red curve). From the presented values, it is clear that the entire frequency range up to 10 MHz can be loaded with a minimum 4-QAM constellation. The actual bit and energy loading used for the 42.3 Mbps result is presented in black lines in the same figure. The optimal constellation size and energy for each subcarrier is determined using an adaptive bit and energy loading algorithm based on the work of Levin and Campello [19]. The received constellations presented in Fig.

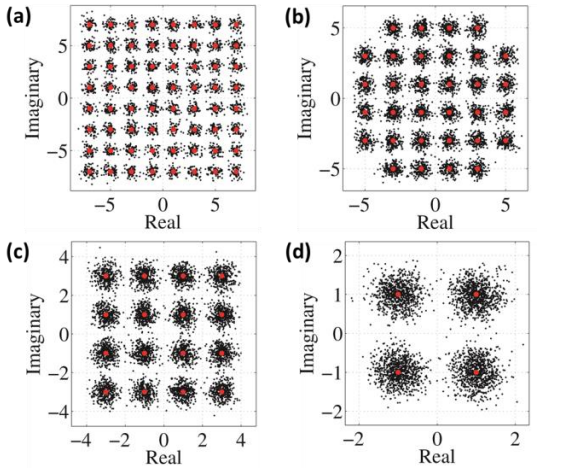

Fig. 4. (a)-(d) examples of the received constellations of the solar cell for R_C = 35 Ω and R_L = 200 Ω.

4 clearly illustrate that the system does not experience any unanticipated distortion effects.

There are two main factors which may limit the data rates of the organic solar cells. These are the low drift mobility of the organic materials, and the time required to discharge the solar cell through the load resistor. In order to further improve the data rates, it is important to understand which factor is dominant in this case. The transit time for the charges to travel across the active layer is given by $\tau_{\mathrm{TRAN}} = d / \mu E = d^2 / \mu V$, where d is the thickness of the active layer, μ is the hole mobility, E is the electrical field and V is the cell voltage. For a load resistance of 600 Ω, the measured cell voltage was 0.51 V. Taking the reported value of μ of 1.7×10^{-3} $cm^2V^{-1}s^{-1}$ [20] gives a transit time of 83 ns. The time required to discharge the solar cell through the load resistor, or so-called RC time constant, is given by $\tau_{\mathrm{RC}} = (R_S + R_L)C = (R_S + R_L)\varepsilon_0\varepsilon_r S / d$. R_L is the load resistance and ε_0 is the vacuum permittivity. The capacitance of the solar cell is determined by the thickness d of the active layer, the relative permittivity ε_r of the active layer and the area S of the device pixel. Taking ε_r = 2 for a wavelength of 658 nm [15] gives an RC time constant of 2.4 μs. This is much longer than the transit time, so the receiver performance is limited by the RC time constant.

In summary we have demonstrated a VLC link using an organic solar cell as the receiver. Such a receiver operates without an external bias and is able to simultaneously communicate data and harvest power. To the best of our knowledge, this is the first reported work using an organic solar cell to achieve energy harvesting and data communication at the same time. The VLC link was tested using adaptive OFDM. The load resistor in the energy harvesting circuit branch can strongly affect the data rates of the VLC link. The maximum data-rate achieved was 42.3 Mbps with a BER of 1.10×10^{-3}. The load resistor also affects the amount of power generated. However, it was found that the communication circuit branch has no negative effect on the power generation. The maximum power output from the solar cell with 8 mm^2 active area was 0.43 mW, and the corresponding data-rate was 34.2 Mbps with a BER of 4.08×10^{-4}. The RC time constant of the solar cell was found to limit the data-rate. This work demonstrates the great potential of organic solar cells for optical wireless communication.

Engineering and Physical Sciences Research Council (EPSRC) (EP/K00042X/1; EP/K008757/1; EP/I00243X/1).

†These authors contributed equally to this work.

See Supplement 1 for supporting content.

REFERENCES

1. M. Z. Afgani, H. Haas, H. Elgala and D. Knipp, in Proceedings of the 2nd International Conference on Testbeds and Research Infrastructures for the Development of Networks and Communities 2006 (Barcelona, Spain, 2006), p. 134.
2. A. M. Khalid, G. Cossu, R. Corsini, P. Choudhury and E. Ciaramella, IEEE Photon. J. 4, 1465-1473 (2012).
3. G. Cossu, A. M. Khalid, P. Choudhury, R. Corsini and E. Ciaramella, Opt. Express 20, B501-B506 (2012).
4. D. Tsonev, C. Hyunchae, S. Rajbhandari, J. J. D. McKendry, S. Videv, E. Gu, M. Haji, S. Watson, A. E. Kelly, G. Faulkner, M. D. Dawson, H. Haas and D. O'Brien, IEEE Photon. Technol. Lett. 26, 637-640 (2014).
5. H. Elgala, R. Mesleh and H. Haas, IEEE Commun. Mag. 49, 56-62 (2011).
6. Z. Wang, D. Tsonev, S. Videv and H. Haas, in Proceedings of IEEE International Conference on Communications (ICC) 2014 (Sydney, Australia, 2014), p. 3348-3353.
7. Z. Wang, D. Tsonev, S. Videv and H. Haas, IEEE J. Sel. Areas Comm., accepted (2105) DOI 10.1109/JSAC.2015.2391811
8. F. C. Krebs , N. Espinosa , M. Hösel , R. R. Søndergaard and M. Jørgensen, Adv. Mater. 26, 29-39 (2014).
9. C. Hyunchae, P. Manousiadis, S. Rajbhandari, D. A. Vithanage, G. Faulkner, D. Tsonev, J. J. D. McKendry, S. Videv, X. Enyuan, G. Erdan, M. D. Dawson, H. Haas, G. A. Turnbull, I. D. W. Samuel and D. C. O'Brien, IEEE Photon. Technol. Lett. 26, 2035-2038 (2014).
10. M. T. Sajjad, P. P. Manousiadis, C. Orofino, D. Cortizo-Lacalle, A. L. Kanibolotsky, S. Rajbhandari, D. Amarasinghe, H. Chun, G. Faulkner, D. C. O'Brien, P. J. Skabara, G. A. Turnbull and I. D. W. Samuel, Adv. Opt. Mater., 3, 536-540 (2015).
11. N. J. Findlay, J. Bruckbauer, A. R. Inigo, B. Breig, S. Arumugam, D. J. Wallis, R. W. Martin and P. J. Skabara, Adv. Mater. 26, 7290-7294 (2014).
12. P. A. Haigh, Z. Ghassemlooy, L.-M. Hoa, S. Rajbhandari, F. Arca, S. F. Tedde, O. Hayden and I. Papakonstantinou, J. Lightwave Technol. 30, 3081-3088 (2012).
13. Z. Ghassemlooy, P. A. Haigh, F. Arca, S. F. Tedde, O. Hayden, I. Papakonstantinou and S. Rajbhandari, Photon. Res. 1, 65-68 (2013).
14. Y. Liang, Z. Xu, J. Xia, S.-T. Tsai, Y. Wu, G. Li, C. Ray and L. Yu, Adv. Mater. 22, E135-E138 (2010).
15. Z. He, C. Zhong, S. Su, M. Xu, H. Wu and Y. Cao, Nat. Photonics 6, 591-595 (2012).
16. G. J. Hedley, A. J. Ward, A. Alekseev, C. T. Howells, E. R. Martins, L. A. Serrano, G. Cooke, A. Ruseckas and I. D. W. Samuel, Nat. Commun. 4, 2867 (2013).
17. M. A. Stosovic, D. Lukac, I. Litovski and V. Litovski, in Proceedings of 11th Symposium on Neural Network Applications in Electrical Engineering 2012 (Belgrade, Serbia, 2012), p. 259-264.
18. P. Rueda, E. Fernandez Lisbona and M. Diez Herrero, in Proceedings of 3rd World Conference on Photovoltaic Energy Conversion 2003 (Osaka, Japan, 2003), p. 817-820.
19. J. Campello, Proceedings of IEEE International Symposium on Information Theory, 1998 (Cambridge, 1998), p. 193.
20. Z. He, C. Zhong, X. Huang, W.-Y. Wong, H. Wu, L. Chen, S. Su and Y. Cao, Adv. Mater. 23, 4636-4643 (2011)